THE JOURNAL OF PHYSICAL CHEMISTRY Letters

LETTER

pubs.acs.org/JPCL

Simulating Dye-Sensitized TiO_2 Heterointerfaces in Explicit Solvent: Absorption Spectra, Energy Levels, and Dye Desorption

Filippo De Angelis,*[,†] Simona Fantacci,[†,‡] and Ralph Gebauer*[,§,∥]

[†]Istituto CNR di Scienze e Tecnologie Molecolari (ISTM), c/o Dipartimento di Chimica, Università di Perugia, via Elce di Sotto 8, I-06123, Perugia, Italy

[‡]Center for Biomolecular Nanotechnology, Italian Institute of Technology (IIT), Via Barsanti, I-73010, Arnesano, Lecce, Italy

[§]The Abdus Salam International Centre for Theoretical Physics (ICTP), Strada Costiera 11, I-34151 Trieste, Italy.

[∥]Istituto Officina dei Materiali, CNR-IOM DEMOCRITOS, I-34136 Trieste, Italy

Supporting Information

ABSTRACT: Dye-sensitized solar cells (DSCs) represent a valuable, efficient, and low-cost alternative to conventional semiconductor photovoltaic devices. A deeper understanding of the dye/semiconductor heterointerface and of the dye-sensitized semiconductor/electrolyte interactions are fundamental for further progress in DSC technology. Here we report an ab initio molecular dynamics simulation of a dye-sensitized TiO_2 heterointerface "immersed" in an explicit water environment for an efficient organic dye, followed by TDDFT excited state calculations of the coupled dye/semiconductor/solvent system. This new computational protocol and the extended model system allows us to gain unprecedented insight into the excited state changes occurring for the solvated dye-sensitized heterointerface at room temperature, and to provide an atomistic picture of water-mediated dye desorption.

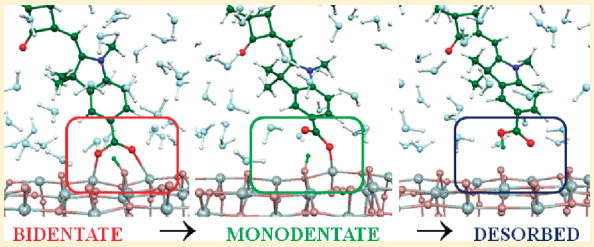

SECTION: Energy Conversion and Storage

Considerable attention and extensive research efforts have been devoted over the last years to dye-sensitized solar cells (DSCs)[1−3] as valuable and low-cost alternatives to silicon and other inorganic semiconductor-based photovoltaic devices. In DSCs, a sensitizing dye adsorbed at the surface of a wide band gap semiconductor (usually nanostructured TiO_2) absorbs light to transfer an electron to the semiconductor conduction band, followed by dye regeneration by a solution redox electrolyte or a solid hole conductor (Scheme 1). Up to now, Ru(II)-polypyridyl sensitizers have shown the highest DSC performances,[4,5] with solar energy-to-electricity conversion efficiencies exceeding 11%.[5] More recently, fully organic dyes have attracted growing interest, due to their easily tunable optical properties, high extinction coefficients and environmental benefits.[6−10] Among the various classes of organic sensitizers, squaraines have been extensively investigated because of their strong absorption bands ($\varepsilon \sim 150.000\ M^{-1}\ cm^{-1}$) in the far red to near-IR spectral regions.[10] Although comparable efficiency to that of Ru(II) dyes has been achieved, the long-term cell stability remains a main issue for organic dyes. A deeper understanding of the dye/semiconductor heterointerface and of the dye-sensitized semiconductor/electrolyte interactions are fundamental for further progress in DSC technology.

In particular, the presence of water in the electrolyte solution is known to be detrimental for the DSC efficiency and temporal stability,[4,11−15] so that DSC sealing techniques have to be elaborated, increasing fabrication costs. Dye desorption and ligand exchange reactions are among the main issues related to water contamination,[4,11−14] although electrode modifications by contact with water have also been reported,[12−14] influencing both the position of the TiO_2 conduction band and recombination of

Scheme 1. Schematic Representation of DSC Functioning and Energy Levels

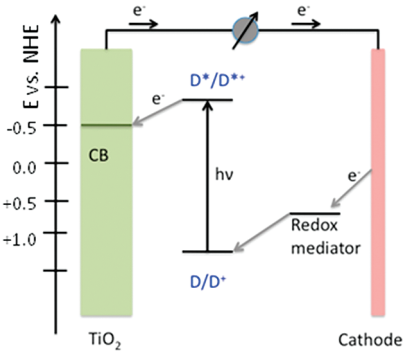

Received: February 9, 2011
Accepted: March 10, 2011
Published: March 16, 2011

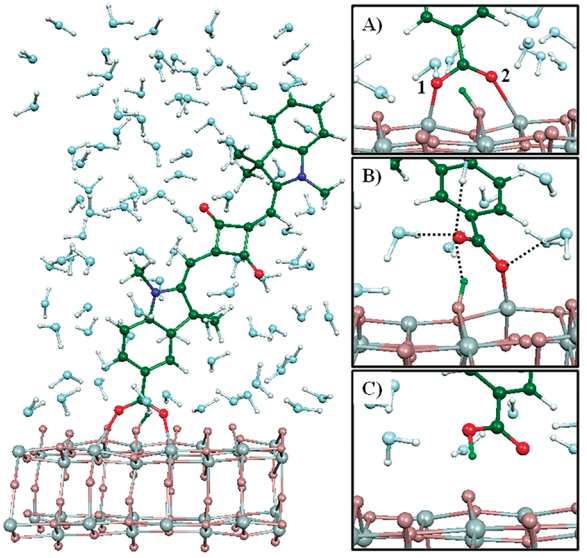

Figure 1. Left: the squaraine dye adsorbed onto a 1 × 4 anatase slab, surrounded by 90 water molecules. Right: Relevant configurations sampled during the dynamics: (A) starting bridged bidentate configuration, and oxygen atoms labels; (B) monodentate configuration; (C) dissociated dye. Notice the different proton positions (green) in A, B, and C. Dashed lines in B represent hydrogen bonds to the carboxylic group.

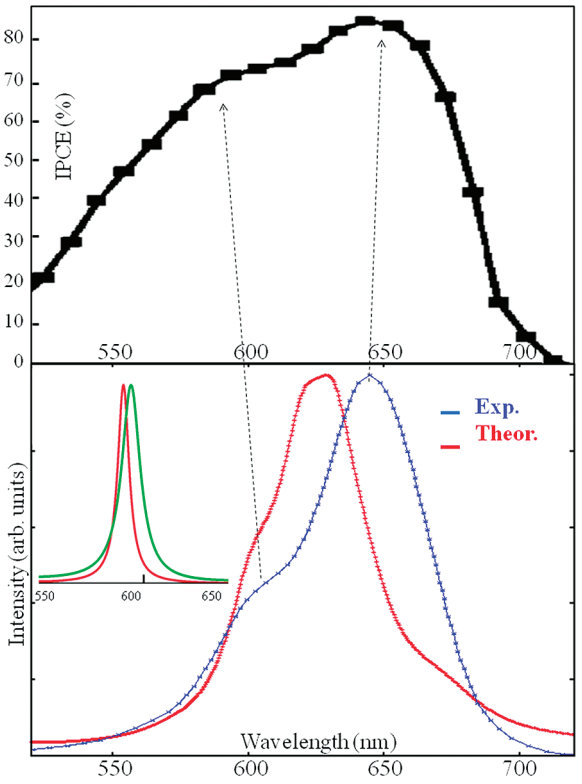

Figure 2. Top: Incident photon-to-current efficiency (IPCE) for a DSC employing the investigated squaraine dye. Adapted from ref 10. Bottom: Comparison between the calculated (blue) and experimental (red) absorption spectra (eV) of the squaraine/TiO_2/water system. The intensity of the experimental spectrum has been rescaled to match the calculated absorption maximum. The dashed arrows indicate the contribution of the absorption features to the IPCE curve. Inset: Calculated absorption spectra at 0 temperature (green without solvent, red with solvent).

injected electrons with the electrolyte.[15] Very recently, however, Law et al. have reported good performance for DSCs employing water-based electrolytes,[16] further stimulating the interest toward understanding the role of water in DSC.

Here we report an *ab initio* molecular dynamics simulation of a dye-sensitized TiO_2 surface "immersed" in an explicit water environment, followed by extensive TDDFT excited state calculations. Ab initio molecular dynamics simulations of model dye/semiconductor heterointerfaces, including non adiabatic excited state dynamics, have been previously reported by Prezhdo and co-workers,[17−20] but solvation effects were not taken into account, although a recent study by the same group reported on "wet electrons" on TiO_2 surfaces.[20] By exploiting a recently developed TDDFT algorithm[21−23] in conjunction with the realistic simulated system, we are able to gain insight into the excited state modifications occurring for the solvated dye-sensitized heterointerface, which are responsible for the high observed photon conversion efficiencies, and to provide an atomistic picture of water-mediated dye desorption. The chosen model system consists of a recently reported squaraine dye,[10] anchored to a 1 × 4 TiO_2 anatase slab exposing the majority (101) surface,[24] surrounded by 90 water molecules (Figure 1).

The initial configuration was first optimized for the system in the absence of solvent,[25] with the dye binding to TiO_2 in a bidentate configuration and a dye proton being transferred to the surface (panel A in Figure 1). Starting from this configuration, the system's dynamics were followed using Car−Parrinello (CP) molecular dynamics,[26] employing the PBE functional.[27] After 1 ps equilibration at 320 K, the system was allowed to evolve naturally in time for 14.5 ps (for further computational details, see Supporting Information).

The initial stages of the dynamics, up to ca. 6 ps, are characterized essentially by solvent and dye fluctuations, along with water adsorption to the TiO_2 surface. A maximum of two water molecules bind simultaneously through their oxygen atoms to surface uncoordinated Ti(IV) centers, out of the six available sites (two sites are occupied by the dye). This data is in agreement with previous studies on the adsorption of water on anatase (101) TiO_2 surfaces, showing that the formation of a submonolayer of water on the surface is energetically favored.[24,28] In the present case, the fact that only two water molecules bind to the surface might also be related to solvation of the dye, which stabilizes outer-sphere waters compared to surface adsorbed ones. We also notice that the observed water adsorption to the TiO_2 surface is consistent with water exerting a blocking function toward recombination of injected electrons with oxidized species in the electrolyte,[11] whereby the adsorbed water molecules and possibly their water overlayers[28] would impede oxidized species in the electrolyte to contact the TiO_2 surface.

During the first 6 ps we sampled 35 configurations at equal time intervals of 0.18 ps, on which we calculated the full TDDFT absorption spectrum of the entire system, Figure 2. This computational protocol marks a new approach compared to previous dynamical investigations of dye-sensitized heterointerfaces[29,30] and excited states of small molecules in solution,[31] allowing us to perform excited state calculations on exactly the same system (dye/semiconductor/solvent) for which the dynamics is computed.

The calculated absorption spectrum for the squaraine-sensitized TiO_2 is compared to experimental data in Figure 2. As it can

dx.doi.org/10.1021/jz200191u |*J. Phys. Chem. Lett.* 2011, 2, 813–817

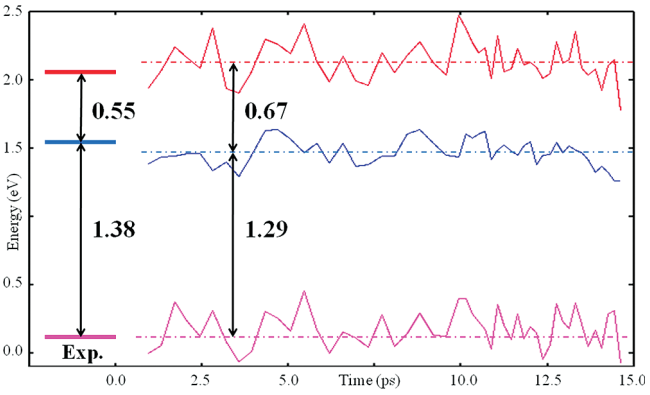

Figure 3. Time (ps) evolution of the excited state oxidation potential (red), TiO_2-based LUMO (blue), and dye-based HOMO (magenta) energies in eV. The zero of the energy scale is set to the value of the HOMO energy of the starting configuration. Dashed lines represent average values of the three quantities. Also shown on the left are experimental spectro-electrochemical data from refs 10 and 32.

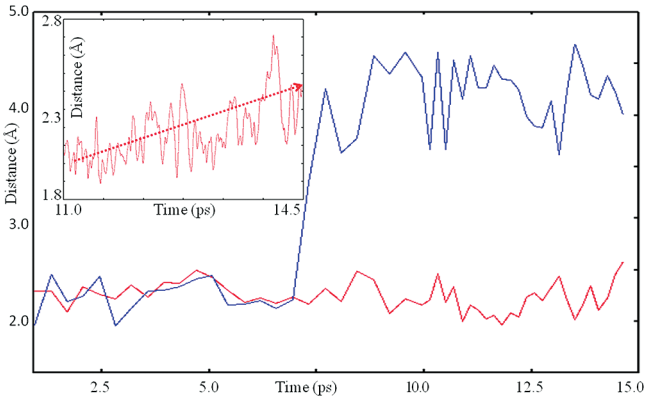

Figure 4. Time (ps) evolution of the carboxylic oxygen−surface titanium atom distances (Å) over the entire simulation range (O1−Ti, blue; O2−Ti, red). Inset: evolution of the short O−Ti distance in the last 3.5 ps of simulation. The arrow is a best fit regression to the running average value of the distance in this time slice.

be noticed, our thermally averaged calculated data are in excellent agreement in terms of absorption maximum wavelength (630 vs 642 nm) and band shape with the experimental data on TiO_2 (Figure 2) and in ethanol solution (Supporting Information).[10] The absorption intensity is mainly originated by dye→dye excitations with small contributions of unoccupied TiO_2 states,[25] while direct dye→TiO_2 excitations, with an onset at ca. 950 nm, are correctly calculated to have a negligible intensity. Our calculations nicely reproduce the experimental spectrum's asymmetry, with a high-energy shoulder that is enhanced upon dye adsorption on TiO_2 (Supporting Information). Such a feature is absent in the zero-temperature calculated spectrum (Figure 2 inset), and is therefore attributed to thermal distortions in the systems' geometry, which are further enhanced on TiO_2. We believe that, beyond thermal and solvent fluctuations, the presence of dye/TiO_2 interactions through the carboxylic group contribute to the observed effect. The dye excited states have a sizable contribution from the carboxylic groups,[10,25] so that upon binding to TiO_2 some perturbation is to be expected. Thus, thermal and solvent fluctuations, along with specific dye interactions with the TiO_2 surface are responsible of the observed behavior. Most notably, the high-energy spectral feature significantly contributes to the incident photon to current conversion efficiency (IPCE in Figure 2), providing additional current generation and DSC efficiency.

With reference to Scheme 1, we further investigated the time evolution of the main energy levels during the dynamics simulation by looking at the highest occupied molecular orbital (HOMO; dye-based), lowest unoccupied molecular orbital (LUMO; TiO_2-based), and excited state energies of the combined system. The sum of the HOMO and absorption maxima energies is an approximation to the dye excited state oxidation potential,[32] (D^*/D^{*+} in Scheme 1) while the LUMO energy represents the bottom of the TiO_2 conduction band (CB). Thus the difference between the dye excited state potential and the bottom of the TiO_2 CB represents the driving force for dye excited state electron injection into the manifold of unoccupied TiO_2 states. By plotting this data as a function of the simulation time (Figure 3), we observe energy fluctuations on the picosecond time scale of the order of 0.4 eV, which are more pronounced for dye-based quantities than for the TiO_2 CB edge. The calculated averages of the HOMO, LUMO, and excited state energies are compared to available experimental data in Figure 3.

The positioning of the TiO_2 CB edge relative to the dye-based HOMO is accurately reproduced. Furthermore, an average driving force for electron injection of 0.67 eV is calculated, in good agreement with the measured alignment of energy levels in such system, which provided a 0.55 V difference.[10] The slight computational overestimate might be due to the fact that we consider the spectrum absorption maximum and not the E_{0-0} to estimate the dye excited state energy.[32] What is important to notice is that the dye excited state is always at least 0.5 eV above the TiO_2 CB edge, despite the thermal fluctuations, ensuring dye excited state coupling to a high density of TiO_2 unoccupied states, thereby a very efficient electron injection process. This is consistent with the high IPCE of ca. 85% measured for this system[10] (Figure 2). The observed behavior is distinctively different from that found for alizarin-sensitized TiO_2 where "in and out" motion of the dye excited states at the edge of the TiO_2 CB triggered the electron injection.[17,18] The important role of fluctuations in the level alignment at the water/TiO_2 interface has also been stressed in recent ab initio molecular dynamics studies.[33,34]

Most notably, after ~6 ps of simulation, we observed a strong solvent reorganization taking place around the TiO_2-bound carboxylic group, which subsequently led to a transition from the starting bridged bidentate configuration to a monodentate adsorption mode (panel B in Figure 1), with one proton still bound to TiO_2. This adsorption change can be visualized by inspecting the time evolution of the relevant O−Ti distances (Figure 4). The two O−Ti distances oscillate around the same value (2.15 Å) up to about 6 ps, when one of the two distances (O1−Ti in Figure 4) suddenly increases to about 4 Å, signaling the detachment of one carboxylic oxygen from the surface. The ensuing monodentate-bound carboxylate is subject to a strong hydrogen-bonding field, with protons from three water molecules and the surface proton within 1.7 Å (panel B in Figure 1), which leads to stabilization of this configuration with respect to the starting bidentate adsorption mode. This carboxylate monodentate configuration, also found to be energetically favored for formic acid adsorption on (101) anatase TiO_2 in the presence of water,[35] is stable for about 6 ps. After this time slice, the surface-bound proton is transferred to the anionic carboxylic group. The dye/TiO_2 interaction, taking place now only via the

dx.doi.org/10.1021/jz200191u |J. Phys. Chem. Lett. 2011, 2, 813–817

monodentate-bound carbonyl oxygen, is substantially weakened, leading to dye desorption toward the end of the simulation (panel C in Figure 1).

This is clear by looking at the inset of Figure 4, which shows the time evolution of the bound O2−Ti distance in the 11−14.5 ps time slice. As it can be noticed, concomitantly to the proton transfer to the dye (∼ 12 ps), an average lengthening of the O2−Ti distance is observed, with fluctuations up to 2.75 Å. As a matter of fact, previous calculations of formic acid adsorption on (101) anatase TiO_2 have shown a sizable reduction of this carboxylic acid adsorption energy to the surface in the presence of water.[35] Separate calculations performed here have shown that adsorption of a single dye molecule in vacuo leads to an energy stabilization of 0.92 eV. A single water molecule binds to TiO_2 with an energy of 0.74−0.71 eV,[24,36] depending on the TiO_2 model. Here we calculate 0.66 eV per molecule for adsorption of a water monolayer to the present TiO_2 model. Thus, dye desorption is the results of the competition between the dye and the solvent for binding to the unsaturated surface Ti(IV) sites and the weakening of dye/TiO_2 interactions, due to dye solvation.

The overall picture extracted from our simulations allows us to assign a precise role to water in the deterioration of DSC devices, stabilizing, prior to dye desorption, a monodentate adsorption mode with respect to a bidentate configuration, the latter ensuring a firmer dye anchoring onto the semiconductor surface. It is also very interesting to note that surface-bound protons assist dye binding to the TiO_2 surface, possibly by increasing the surface dipolar field, since upon protonation of the monodentate carboxylate group we observe dye desorption from the surface. This also highlights that the acidity of the dye anchoring group(s) plays a fundamental role in stabilizing dye adsorption to TiO_2 through surface protonation, thereby casting an additional design strategy for new dyes with improved functioning in DSC devices.

In summary, we have reported an extensive ab initio molecular dynamics simulation of a dye-sensitized heterointerface in the presence of an explicit water environment, including thermally averaged excited state calculations. Our results reproduce the spectral modifications occurring upon dye adsorption onto TiO_2 and allow us to quantify the effect of thermal fluctuations on the dye/semiconductor energy alignment, which are both related to the optimal photocurrent generation for DSC employing the investigated squaraine dye. We also provide an atomistic picture of water-mediated dye desorption from the semiconductor surface, thus providing a deeper understanding of the crucial heterointerface for DSCs functioning and stability.

■ ASSOCIATED CONTENT

Supporting Information. Computational details. Absorption spectra. This information is available free of charge via the Internet at http://pubs.acs.org/.

■ AUTHOR INFORMATION

Corresponding Author

*E-mail: filippo@thch.unipg.it, rgebauer@ictp.it.

■ ACKNOWLEDGMENT

We thank the DEISA Consortium (www.deisa.eu), cofunded through the EU FP6 project RI-031513 and the FP7 project RI-222919, for support within the DEISA Extreme Computing Initiative. F.D.A. and S.F. thank IIT-SEED 2009 - project HELYOS and FP7-ENERGY 2010 project ESCORT - 261920, for financial support.

■ REFERENCES

(1) O'Regan, B.; Grätzel, M. A Low-Cost, High-Efficiency Solar Cell Based on Dye-Sensitized Colloidal Titanium Dioxide Films. *Nature* **1991**, *353*, 737–40.

(2) Hagfeldt, A.; Grätzel, M. Light-Induced Redox Reactions in Nanocrystalline Systems. *Chem. Rev.* **1995**, *95*, 49–68.

(3) Grätzel, M. Photoelectrochemical Cells. *Nature* **2001**, *414*, 338–344.

(4) Nazeeruddin, M. K.; Kay, A.; Rodicio, I.; Humphry-Baker, R.; Muller, E.; Liska, P.; Vlachopoulos, N.; Grätzel, M. Conversion of Light to Electricity by cis-X_2Bis(2,2′-bipyridyl-4,4′-dicarboxylate)ruthenium-(II) Charge-Transfer Sensitizers (X = Cl^-, Br^-, I^-, CN^-, and SCN^-) on Nanocrystalline Titanium Dioxide Electrodes. *J. Am. Chem. Soc.* **1993**, *115*, 6382–6390.

(5) Nazeeruddin, M. K.; De Angelis, F.; Fantacci, S.; Selloni, A.; Viscardi, G.; Liska, P.; Ito, S.; Takeru, B.; Grätzel, M. Combined Experimental and DFT-TDDFT Computational Study of Photoelectrochemical Cell Ruthenium Sensitizers. *J. Am. Chem. Soc.* **2005**, *127*, 16835–16847.

(6) For a review, see Mishra, A.; Fischer, M. K. R.; Bäuerle, P. Metal-Free Organic Dyes for Dye-Sensitized Solar Cells: From Structure: Property Relationships to Design Rules. *Angew. Chem., Int. Ed.* **2009**, *48*, 2474–2499.

(7) Ito, S.; Zakeeruddin, S. M.; Humphry-Baker, R.; Liska, P.; Charvet, R.; Comte, P.; Nazeeruddin, M. K.; Péchy, P.; Takata, M.; Miura, H.; Uchida, S.; Grätzel, M. High-Efficiency Organic-Dye-Sensitized Solar Cells Controlled by Nanocrystalline-TiO_2 Electrode Thickness. *Adv. Mater.* **2006**, *18*, 1202–1205.

(8) Ito, S.; Miura, H.; Uchida, S.; Takata, M.; Sumioka, K.; Liska, P.; Comte, P.; Pechy, P.; Grätzel, M. High-Conversion-Efficiency Organic Dye-Sensitized Solar Cells with a Novel Indoline Dye. *Chem. Commun.* **2008**, 5194–5196.

(9) Zhang, G.; Bala, H.; Cheng, Y.; Shi, D.; Lv, X.; Yu, Q.; Wang, P. High Efficiency and Stable Dye-Sensitized Solar Cells with an Organic Chromophore Featuring a Binary π-Conjugated Spacer. *Chem. Commun.* **2009**, 2198–2200.

(10) Yum, J-.H.; Walter, P.; Huber, S.; Rentsch, D.; Geiger, T.; Nüesch, F.; De Angelis, F.; Grätzel, M.; Nazeeruddin, M. K. Efficient Far Red Sensitization of Nanocrystalline TiO_2 Films by an Unsymmetrical Squaraine Dye. *J. Am. Chem. Soc.* **2007**, *129*, 10320–10321.

(11) Liu, Y.; Hagfeldt, A.; Xiao, X. R.; Lindquist, S. E. Investigation of Influence of Redox Species on the Interfacial Energetics of a Dye-Sensitized Nanoporous TiO_2 Solar Cell. *Sol. Energy Mater. Sol. Cells* **1998**, *55*, 267–281.

(12) Zakeeruddin, S.; Nazeeruddin, M. K.; Humphry-Baker, R.; Barolo, C.; Viscardi, G.; Grätzel, M.; Nazeeruddin, M. K. Design, Synthesis, and Application of Amphiphilic Ruthenium Polypyridyl Photosensitizers in Solar Cells Based on Nanocrystalline TiO_2 Films. *Langmuir* **2002**, *18*, 952–954.

(13) Jung, Y. S.; Yoo, B.; Lim, M. K.; Lee, S. Y.; Kim, K. J. Effect of Triton X-100 in Water-Added Electrolytes on the Performance of Dye-Sensitized Solar Cells. *Electrochim. Acta* **2009**, *54*, 6286–6291.

(14) Mikoshiba, S.; Muari, S.; Sumino, H.; Kado, T.; Kosugi, D.; Hayase, S. Ionic Liquid Type Dye-Sensitized Solar Cells: Increases in Photovoltaic Performances by Adding a Small Amount of Water. *Curr. Appl. Phys.* **2005**, *5*, 152–158.

(15) Kroeze, J. E.; Hirata, N.; Koops, S.; Nazeeruddin, M. K.; Schmidt-Mende, L.; Grätzel, M.; Durrant, J. R. Alkyl Chain Barriers for Kinetic Optimization in Dye-Sensitized Solar Cells. *J. Am. Chem. Soc.* **2006**, *128*, 16376–16383.

(16) Law, C.; Pathirana, S. C.; Li, X.; Anderson, A. Y.; Barnes, P. R.; Listorti, A.; Ghaddar, T. H.; O'Regan, B. C. Water-Based Electrolytes for Dye-Sensitized Solar Cells. *Adv. Mater.* **2010**, *22*, 4505–4509.

(17) Duncan, W. R.; Stier, W. M.; Prezhdo, O. V. Ab Initio Nonadiabatic Molecular Dynamics of the Ultrafast Electron Injection across the Alizarin−TiO_2 Interface. *J. Am. Chem. Soc.* **2005**, *121*, 7941–7951.

(18) Duncan, W. R.; Craig, C. F.; Prezhdo, O. V. Time-Domain Ab Initio Study of Charge Relaxation and Recombination in Dye-Sensitized TiO_2. *J. Am. Chem. Soc.* **2007**, *129*, 8523–8528.

(19) Duncan, W. R.; Prezhdo, O. V. Temperature Independence of the Photoinduced Electron Injection in Dye-Sensitized TiO_2 Rationalized by Ab Initio Time-Domain Density Functional Theory. *J. Am. Chem. Soc.* **2008**, *130*, 9756–9762.

(20) Fischer, S. A.; Duncan, W. R.; Prezhdo, O. V. Ab Initio Nonadiabatic Molecular Dynamics of Wet-Electrons on the TiO_2 Surface. *J. Am. Chem. Soc.* **2009**, *131*, 15483–15491.

(21) Rocca, D.; Gebauer, R.; Saad, Y.; Baroni, S. Turbo Charging Time-Dependent Density-Functional Theory with Lanczos Chains. *J. Chem. Phys.* **2008**, *128*, 154105.

(22) Walker, B.; Gebauer, R. Ultrasoft Pseudopotentials in Time-Dependent Density-Functional Theory. *J. Chem. Phys.* **2007**, *127*, 164106.

(23) Walker, B.; Gebauer, R.; Saitta, A. M.; Baroni, S. Efficient Approach to Time-Dependent Density-Functional Perturbation Theory for Optical Spectroscopy. *Phys. Rev. Lett.* **2006**, *96*, 113001.

(24) Vittadini, A.; Selloni, A.; Rotzinger, F. P.; Gräztel, M. Structure and Energetics of Water Adsorbed at TiO_2 Anatase (101) and (001) Surfaces. *Phys. Rev. Lett.* **1998**, *81*, 2954–2957.

(25) Rocca, D.; Gebauer, R.; De Angelis, F.; Nazeeruddin, M. K.; Baroni, S. Time-Dependent Density Functional Theory Study of Squaraine Dye-Sensitized Solar Cells. *Chem. Phys. Lett.* **2009**, *475*, 49–53.

(26) Car, R.; Parrinello, M. Unified Approach for Molecular Dynamics and Density-Functional Theory. *Phys. Rev. Lett.* **1985**, *55*, 2471–2474.

(27) Perdew, J. P.; Burke, K.; Ernzerhof, M. Generalized Gradient Approximation Made Simple. *Phys. Rev. Lett.* **1996**, *77*, 3865–3868.

(28) Tilocca, A.; Selloni, A. Vertical and Lateral Order in Adsorbed Water Layers on Anatase TiO_2(101). *Langmuir* **2004**, *20*, 8379–8384.

(29) De Angelis, F.; Fantacci, S.; Selloni, A.; Nazeeruddin, M. K.; Grätzel, M. First-Principles Modeling of the Adsorption Geometry and Electronic Structure of Ru(II) Dyes on Extended TiO_2 Substrates for Dye-Sensitized Solar Cell Applications. *J. Phys. Chem. C* **2010**, *114*, 6054–6061.

(30) Schiffmann, F.; VandeVondele, J.; Hutter, J.; Wirz, R.; Urakawa, A.; Baiekr, A. Protonation-Dependent Binding of Ruthenium Bipyridyl Complexes to the Anatase(101) Surface. *J. Phys. Chem. C* **2010**, *114*, 8398–8404.

(31) Crescenzi, O.; Pavone, M.; De Angelis, F.; Barone, V. Solvent Effects on the UV ($n \rightarrow \pi^*$) and NMR (^{13}C and ^{17}O) Spectra of Acetone in Aqueous Solution. An Integrated Car−Parrinello and DFT/PCM Approach. *J. Phys. Chem. B* **2005**, *109*, 445–453.

(32) De Angelis, F.; Fantacci, S.; Selloni, A. Alignment of the Dye's Molecular Levels with the TiO_2 Band Edges in Dye-Sensitized Solar Cells: A DFT-TDDFT Study. *Nanotechnology* **2008**, *19*, 42002–424009.

(33) Cheng, H.; Selloni, A. Hydroxide Ions at the Water/Anatase TiO_2(101) Interface: Structure and Electronic States from First Principles Molecular Dynamics. *Langmuir* **2010**, *26*, 11518–11525.

(34) Cheng, J.; Sprik, M. Aligning Electronic Energy Levels at the TiO_2/H_2O Interface. *Phys. Rev. B* **2010**, *82*, 081406R.

(35) Vittadini, A.; Selloni, A.; Rotzinger, F. P.; Gräztel, M. Formic Acid Adsorption on Dry and Hydrated TiO_2 Anatase (101) Surfaces by DFT Calculations. *J. Phys. Chem. B* **2000**, *104*, 1300–1306.

(36) Li, W.-K.; Gong, X.-Q.; Lu, G.; Selloni, A. Different Reactivities of TiO_2 Polymorphs: Comparative DFT Calculations of Water and Formic Acid Adsorption at Anatase and Brookite TiO_2 Surfaces. *J. Phys. Chem. C* **2008**, *112*, 6594–6596.